Searching 22 μm Excess Stars in LAMOST DR1 Stellar Catalog

Chao-Jian Wu[1,2], Hong Wu[1,2], Kang Liu, [3], Tan-Da Li[2], Ming Yang[1], Man I Lam [1], Fan Yang[1]

chjwu@bao.ac.cn

Received _____; accepted _____

[1]Key Laboratory of Optical Astronomy, National Astronomical Observatories, Chinese Academy of Sciences Beijing 100012, China

[2]National Astronomical Observatories, Chinese Academy of Sciences, Beijing 100012, China

[3]Department of Astronomy, Beijing Normal University, Beijing, 100875, P. R. China

Abstract

Since the release of LAMOST catalog, we have chance to use LAMOST DR1 catalog to search 22 μm excess stars. Combining with Tycho 2 catalog and WISE All-sky catalog, we obtain 23 stars showing 22 μm excess. Among the 23 stars, 11 are giants, 10 are main sequence stars and 2 are unsure. According to the [Fe/H] provided by LAMOST, we estimated the ages of main sequence stars except for giants, which range from 0.4 to 6.6 Gyr. The SEDs are also fitted with the photometric information from optical to mid infrared band. Most of them show an obvious excess from 12 μm band and one even shows excess from K_s band. All of them are interesting candidates of beris disks for further study.

Subject headings: infrared: stars-planetary systems - stars: formation - planetary systems: protoplanetary disks

1. Introduction

More and more surveys (*IRAS*, *Infrared Space Observatory (ISO)*, *Spitzer Space Telescope*, *Herschel* and *WISE* et al.) have been conducted to search for infrare excess stars (especially the dusty disks and exoplanets system) since the first discovery of the infrared excess phenomenon (known as a debris disk) around Vega(Aumann et al. 1984).

In fact, there are many reasons can cause excess at infrared band (Wu et al. 2013). Infrared exess may be produced by protostars (Thompson 1982) or the surrounding dust disk (Gorlova et al. 2004, 2006; Rhee et al. 2007; Hovhannisyan et al. 2009; Koerner et al. 2010; Wu et al. 2012), or from giant stars. However, the IR excess could also come from the companion star (like white dwarfs + M stars, white dwarfs + brown dwarfs or + dusty disks) (Debes et al. 2011), background galaxy, background nebula or interstellar medium or random foreground object, not from the object itself(Ribas et al. 2012). In our study, we only focus on the first two kinds of stars.

To study the properties of the IR excess stars more in detail, only the photometric information of multiband is not sufficient. We need more information, e.g., spectrum, metallicity, ages and so on. The *Guoshoujing Telescope*, abbreviated as LAMOST, offers an opportunity to study the characteristics of infrared excess stars in LAMOST DR1 Catalog. More detail will be described in Sec 2.1.

While searching the infrared excess stars from LAMOST DR1 Catalog, we also introduce the Wide-field Infrared Survey Explorer (WISE; Wright et al. 2010) All-sky data, the observations at 22 μm will undoubtedly provide an opportunity to search for more IR excess stars in the whole sky (Wu et al. 2012, 2013). Some relative work have been published. Kennedy & Wyatt (2012) described a search for IR excess stars from *Kepler* and *WISE* and concluded that the excesses in the *Kepler* field are mainly due to high background level. Lawler & Gladman (2012) studied the dust emission around more than

900 *Kepler* exoplanet candidates using *WISE* data and they found 8 candidates with IR excess. Morales et al. (2012) studied the dust of 591 planetary systems from Exoplanet Encyclopaedia as of 2012 January 31, 350 can be detected by *WISE* and 9 stars have mid-IR excess. Avenhaus et al. (2012) searched IR excess mainly for M stars. Wu et al. (2013) focused on the bright stars ($V_{mag} \leq 10.27$) and searched more than 70 new identified 22 μm excess stars.

Moreover, we also introduce the Tycho 2 catalog (Høg et al. 2000) to cross-correlate with WISE All-Sky Catalog and LAMOST DR1 Catalog so as to eliminate the effects of QSOs or distant galaxies cantained in the LAMOST Stellar Catalog as point sources. Undoubtedly, this will remove many fainter sources, meanwhile, it also improves the accuracy, see Sec 2.2.

In this paper, we describe the candidate selection criterion, source identification in Section 2. In Section 3, we determine the ages of candidates, show the metallicity, SEDs and other information, also giving some discussion. The conclusion and summary are presented in Section 4.

2. Data

2.1. LAMOST DR1 Stellar Catalog

The first observation mission of the LAMOST regular survey launched on September 28, 2012, and have been already successfully finishied on July 15, 2013. Totally, over 1.2 million spectra with signal to noise larger than 10 of 689 square degrees are obtained. The data set of LAMOST data release one (DR1), including spectra of the pilot survey and spectra of the first year of the regular spectroscopic survey, have already published to domestic data users and foreign partners. The DR1 totally contains 2,204,860 spectra,

including 717,660 spectra of pilot survey and 1,487,200 spectra of regular survey. In the stellar catalog, there are 648,820 stars in pilot survey and 1,295,586 stars in the first year spectroscopic survey. In addition, the stellar catalog contains the atmospheric parameters of 1,085,404 stars, which becomes the largest stellar spectral parameters catalog in the world at present. [1]

2.2. Data Selection

As described above, we used the LAMOST DR1 stellar catalog. In fact, it is a point source catalog and contains the distant galaxies, QSOs et al (like 2MASS point source catalog). While in our work, we concerned only the stars. So it is very important to select the stellar sources from these point sources. Here we introduce Tycho 2 catalog (Høg et al. 2000), the V mag (calculated from V_T mag given in this catalog) can be fainter than 15. So it can be used to help select out most of stars with high photometric precision from LAMOST stellar catalog. In this way, we obtain 65,042 stars, see gray region in Fig 1.

Then we use the matched stellar catalog above to cross-correlate with *WISE* All-Sky Catalog. The matched radius is 6"(Wu et al. 2013). According to the photometric accuracy of the LAMOST DR1 stellar catalog, we only use stars with $S/N \geq 15$ at g band and i band. Selecting those with $S/N \geq 10$ at W4 band, about 1,076 sources are left.

The method of selecting 22 μm excess stars is similar with our previous work (Wu et al. 2013). Gorlova et al. (2004, 2006) provided an approach for searching for IR excess in the mid-IR band using the criterion that the mean $K_s - [24]_{vega}$ (here [24] means the Vega magnitude at 24 μm, and [22] has the same meaning) value should be greater than 0.33 at a 3σ confidence level ($0.33 = 3 \times 0.11$, where 0.11 is the 1σ value). In Hovhannisyan et al.

[1] www.lamost.org

(2009), the criterion was changed slightly to $K_s - [24] \geq 0.2$. Wu et al. (2013) also gave the $K_s - [22]$ criterion for different spectral type with *WISE* W4 band by fitting the histgram of $K_s - [22]$ with a gaussian function. Fig 2 shows the histgram of $K_s - [22]$. To reduce the bias introduced by the small number of matched catalog, we use 4σ confidence for all the 1,076 sources. That means the criterion used in this work is $K_s - [22] \geq 0.43$. After deducting the binary or multiple system effecting and background effecting with *IRAS* 100 μm, we obtain 23 new identified mid-infrared μm excess stars (red points in Fig 1).

3. Analysis and Results

3.1. Hertzsprung Russell Diagram

The separation between main-sequence stars and giants can help us to understand the possible different mechanisms of IR-excess stars. The stellar parameters provided in LAMOST DR1 can help us to separate main-sequence stars and giants. Fig 3 shows the temperature versus log(g) Hertzsprung-Russell (short for H-R) diagram.

From Fig 3 we can see that 11 sources (red points) are giants 10 stars are main sequence stars (blue points)and 2 stars (black asterisks)are unsure. Among the 12 sources (10 main sequence stars and 2 unsure stars), there are 8 F type stars, 2 A type stars, 1 B and 1 G type stars. They are all noted in Table 1. In our work, we are only interested in the main sequence stars with infared excess. So in the next section, we only determined ages for 10 main sequence stars and 2 unsure stars, and also, mainly show the characteristics for the 12 stars.

3.2. Age

Age is an important parameter for studying the IR excess stars such as studying the evolution of fraction luminosity and dust temperature (Wyatt 2008). Zhao et al. (2011) estimates ages of more than 30 binaries containing white dwarf (WD) components by calculating cooling times of the WDs and obtain ages of progenitor stars from clusters. Sierchio et al. (2014) shows three methods to estimate ages: placement on the H-R diagram, chromospheric activity indices and X-ray luminosity. Similar with the first method, we estimate star ages by drawing the isochrones on the H-R diagram. The isochrones are calculated with metallicity given by LAMOST DR1 catalog (Kim et al. 2002). The effects of α-enhancement is considered when calculating isochrones (Kim et al. 2002).

The isochrones are shown in Fig 4. Symbols with the same color means the same α-enhancement. The corresponding solid lines are plotted for estimating ages. As described above, we estimate the ages of 10 stars except for J083717.41+512014.2, J040037.42+323808.1 and 11 giants stars. J083717.41+512014.2 is a G5 star and its age can not be estimated with this method. J040037.42+323808.1 is a B type star, locates in Taurus star formation region and with large bias of [Fe/H] in our catalog. Generally, the age of B type star is within 10 Myr. The lifetime is so short that the dust around is instable because of Poynting-Roberson drag and collisional destruction (Beichman et al. 2005; Rieke et al. 2005; Backman & Paresce 1993; Lagrange et al. 2000; Dominik & Decin 2003; Wu et al. 2012). In the other word, it is almost impossible that there is planet system around B star. So the 22 μm excess of B type stars should be from early dust ($\leq$ 100 Myr) around.

The ages obtained in this work ranges from 0.4 to 6.6 Gyr. In the early 21st Century, debris disks were first found with ages older than 0.4 Gyr (Spangler et al. 2001; Edwards & Stencel 2003). Generally, larger dust grain drifting from Poynting-Robertson drag would be destroyed on a timescale of 110 Myr (Kim et al. 2005). So the IR excess

found in our samples may be from the recently produced dust (Beichman et al. 2005). The recently produced dust could arise primarily from collisions between planetsimals and from cometary activity(Rieke et al. 2005). While for the stars above a Gyr is the delayed onset of collisional cascades by late planet formation far away from the central star (Dominik & Decin 2003). This indicates the probability of existing planetary systems in our samples.

3.3. Other stellar parameters

Fig 5 shows the SEDs of 12 selected main sequence candidates. All these SEDs are fitted with Kurucz models(Robitaille et al. 2007; Kurucz 1979). Here we use 9 bands information to do fitting, B, V (from simbad or Tycho catalog), J, H, K_s (from 2MASS), W1, W2, W3 and W4 (from WISE All-sky catalog). The SEDs provided in this paper can be used to test our $K - [22]$ method of searching for excess IR. All the candidates in Fig 5 show an obvious excess at 22 μm (W4), even at 12 μm band. The up triangular symbols mean flux excess comparing to black body radiation. Some even show excess in the K_s band (**J121148.66+522123.7**) and 3.4 μm (**J064030.57+595430.8, J165446.44+572123.4**), which indicates that they are with hotter dust around than others. There is one early type star (J040037.42+323808.1) with $T_{eff} \sim 24000$(K) in our sample (see Sec 3.2).

Since there is no photometric information at longer band, we do not know the peak of the infrared excess and can not determine whether there are disks around candidates. Therefore, we need far infrared observation to confirm in the future.

The metallicity in this paper was provided by LAMOST DR1 catalog. It is calculated with LAMOST high resolution spectroscopy. As shown in Table 1, the metallicity of main

sequence stars with 22 μm excess ranges from -0.419 to 0.14, but most of them are close to 0, which indicates that they belong to solar type stars. There are four metal poor stars (**J011112.37+345811.9, J075945.89+170817.7, J165446.44+572123.4 and J173710.48+574708.2**). Fig 6 shows the distribution of age *vs* [Fe/H]. Since we can not determine the age of **J083717.41+512014.2** and **J040037.42+323808.1**, there are only 10 stars shown in Fig 6. Dotted line shows the relation between age and metallicity for disk stars (Zhao et al. 2011). The uncertainties are also displayed for comparison. Clearly, **J173710.48+574708.2** is a metal-poor star but with older age.

4. Summary

In this work, we use LAMOST DR1 catalog to search 22 μm excess combining with Tycho 2 catalog and WISE All-sky catalog. The $K_s - [22]$ criterion is used in this paper (Wu et al. 2013). Then we obtain 23 stars with 22 μm excess. Each candidate presented here can be further studied with higher angular resolution infrared imaging or infrared spectroscopy. Among them, 11 are giants and the left 12 stars are the ones we are interested in. According to calculate isochrones using [Fe/H] provided by LAMOST, we estimate the ages of 10 stars except for 2 main sequence stars and giants, which range from 0.4 to 6.6 Gyr. With the photometric information of optical and mid infrared band, the SEDs are fitted. From the SEDs, we find that almost all of them show excess from 12 μ band. There are 3 show obvious excess from 3.4 μm band and one shows slight excess even in the K_s band. Moreover, according to the metallicity provided by LAMOST, we also compare the relation between age and metallicity with precious work (Zhao et al. 2011). There are four stars are metal-poor and one is metal-poor but with older age.

With the further release data of LAMOST, we believe that we can search more mid-infrared excess stars and study the characteristics of them more in detail with such a

wealth of information.

Ch.-J. Wu thanks C. Liu and Y.-F. Huang for valuable discussion and L. Lan for warmhearterd help. This project is supported by the National Natural Science Foundation of China (grant No. 11403061), the China Ministry of Science and Technology under the State Key Development Program for Basic Research (2014CB845705, 2012CB821800), the National Natural Science Foundation of China (grant Nos. 11173030, 11225316, 11078017, 11303038, 10833006, 10978014, and 10773014), the Key Laboratory of Optical Astronomy, National Astronomical Observatories, Chinese Academy of Sciences.

REFERENCES

Aumann, H. H., Beichman, C. A., Gillett, F. C., et al. 1984, ApJ, 278, L23

Avenhaus, H., Schmid, H. M., & Meyer, M. R. 2012, A&A, 548, A105

Backman, D. E. & Paresce, F. 1993, in Protostars and Planets III, ed. E. H. Levy & J. I. Lunine, 1253–1304

Beichman, C. A., Bryden, G., Rieke, G. H., et al. 2005, ApJ, 622, 1160

Debes, J. H., Hoard, D. W., Wachter, S., et al. 2011, ApJS, 197, 38

Dominik, C. & Decin, G. 2003, ApJ, 598, 626

Edwards, M. L. & Stencel, R. E. 2003, in The Future of Cool-Star Astrophysics: 12th Cambridge Workshop on Cool Stars, Stellar Systems, and the Sun, ed. A. Brown, G. M. Harper, & T. R. Ayres, Vol. 12, 754–756

Gorlova, N., Padgett, D. L., Rieke, G. H., et al. 2004, ApJS, 154, 448

Gorlova, N., Rieke, G. H., Muzerolle, J., et al. 2006, ApJ, 649, 1028

Høg, E., Fabricius, C., Makarov, V. V., Urban, S., Corbin, T., Wycoff, G., Bastian, U., Schwekendiek, P., & Wicenec, A. 2000, A&A, 355, L27

Hovhannisyan, L. R., Mickaelian, A. M., Weedman, D. W., et al. 2009, AJ, 138, 251

Kennedy, G. M. & Wyatt, M. C. 2012, MNRAS, 426, 91

Kim, J. S., Hines, D. C., Backman, D. E., et al. 2005, ApJ, 632, 659

Kim, Y.-C., Demarque, P., Yi, S. K., & Alexander, D. R. 2002, ApJS, 143, 499

Koerner, D. W., Kim, S., Trilling, D. E., et al. 2010, ApJ, 710, L26

Kurucz, R. L. 1979, ApJS, 40, 1

Lagrange, A.-M., Backman, D. E., & Artymowicz, P. 2000, Protostars and Planets IV, 639

Lawler, S. M. & Gladman, B. 2012, ApJ, 752, 53

Morales, F. Y., Padgett, D. L., Bryden, G., Werner, M. W., & Furlan, E. 2012, ApJ, 757, 7

Rhee, J. H., Song, I., Zuckerman, B., & McElwain, M. 2007, ApJ, 660, 1556

Ribas, Á., Merín, B., Ardila, D. R., & Bouy, H. 2012, A&A, 541, A38

Rieke, G. H., Su, K. Y. L., Stansberry, J. A., et al. 2005, ApJ, 620, 1010

Robitaille, T. P., Whitney, B. A., Indebetouw, R., & Wood, K. 2007, ApJS, 169, 328

Sierchio, J. M., Rieke, G. H., Su, K. Y. L., & Gáspár, A. 2014, ApJ, 785, 33

Spangler, C., Sargent, A. I., Silverstone, M. D., Becklin, E. E., & Zuckerman, B. 2001, ApJ, 555, 932

Thompson, R. I. 1982, ApJ, 257, 171

Wright, E. L., Eisenhardt, P. R. M., Mainzer, A. K., et al. 2010, AJ, 140, 1868

Wu, C.-J., Wu, H., Lam, M.-I., Yang, M., Wen, X.-Q., Li, S., Zhang, T.-J., & Gao, L. 2013, ApJS, 208, 29

Wu, H., Wu, C.-J., Cao, C., et al. 2012, RAA, 12, 513

Wyatt, M. C. 2008, ARA&A, 46, 339

Zhao, J. K., Oswalt, T. D., Rudkin, M., Zhao, G., & Chen, Y. Q. 2011, AJ, 141, 107

This manuscript was prepared with the AAS LaTeX macros v5.2.

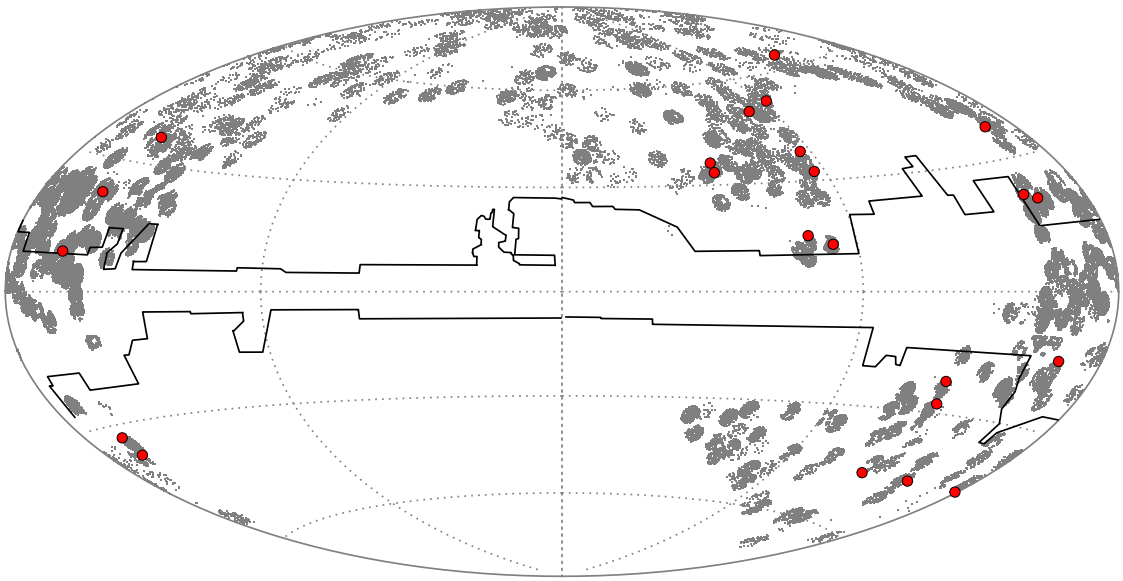

Fig. 1.— Distribution of IR-excess stars in a Galactic Aitoff projection. We show the distribution of the matched catalog from LAMOST DR1 catalog and Tycho2 catalog (gray dots); and the red points are the 23 IR-excess candidates selected in this work. The region between the black solid lines is the star formation region.

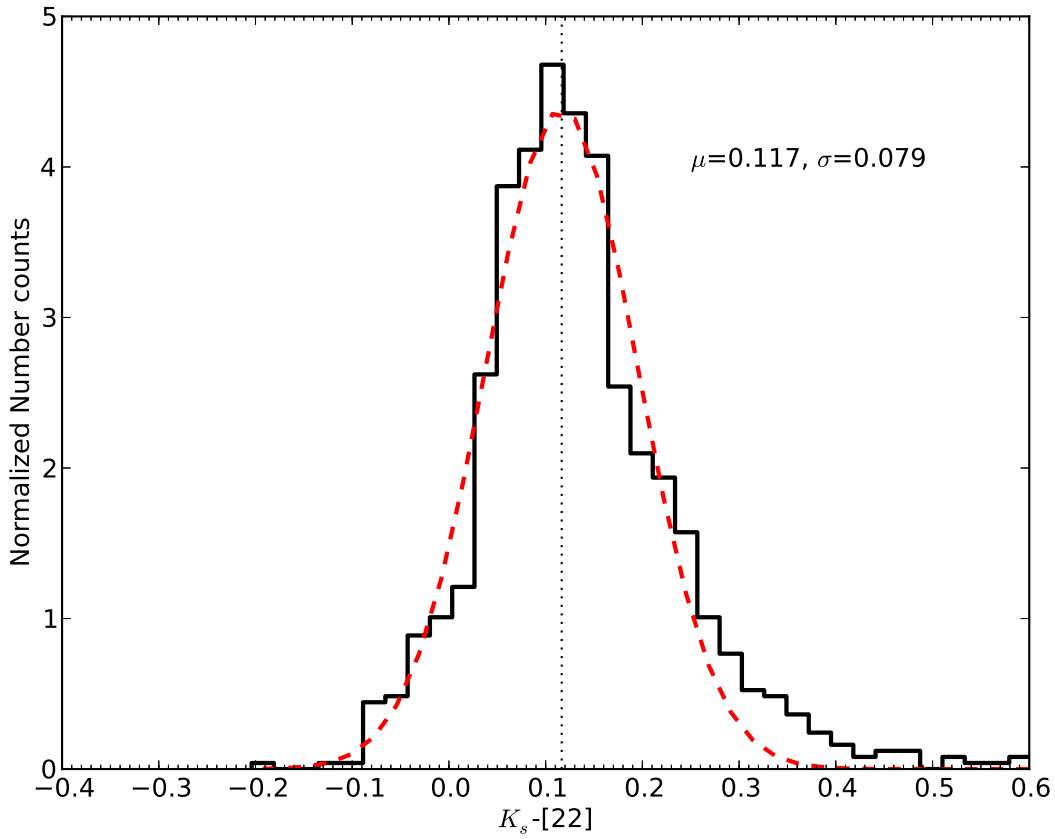

Fig. 2.— Goodness of fit for all matched sources. The criterion is $K_s - [22]_{\mu m} \geq \mu + 4\sigma = 0.43$, which means that those with $K_s - [22]_{\mu m} \geq 0.43$ are identified as 22 μm excess stars.

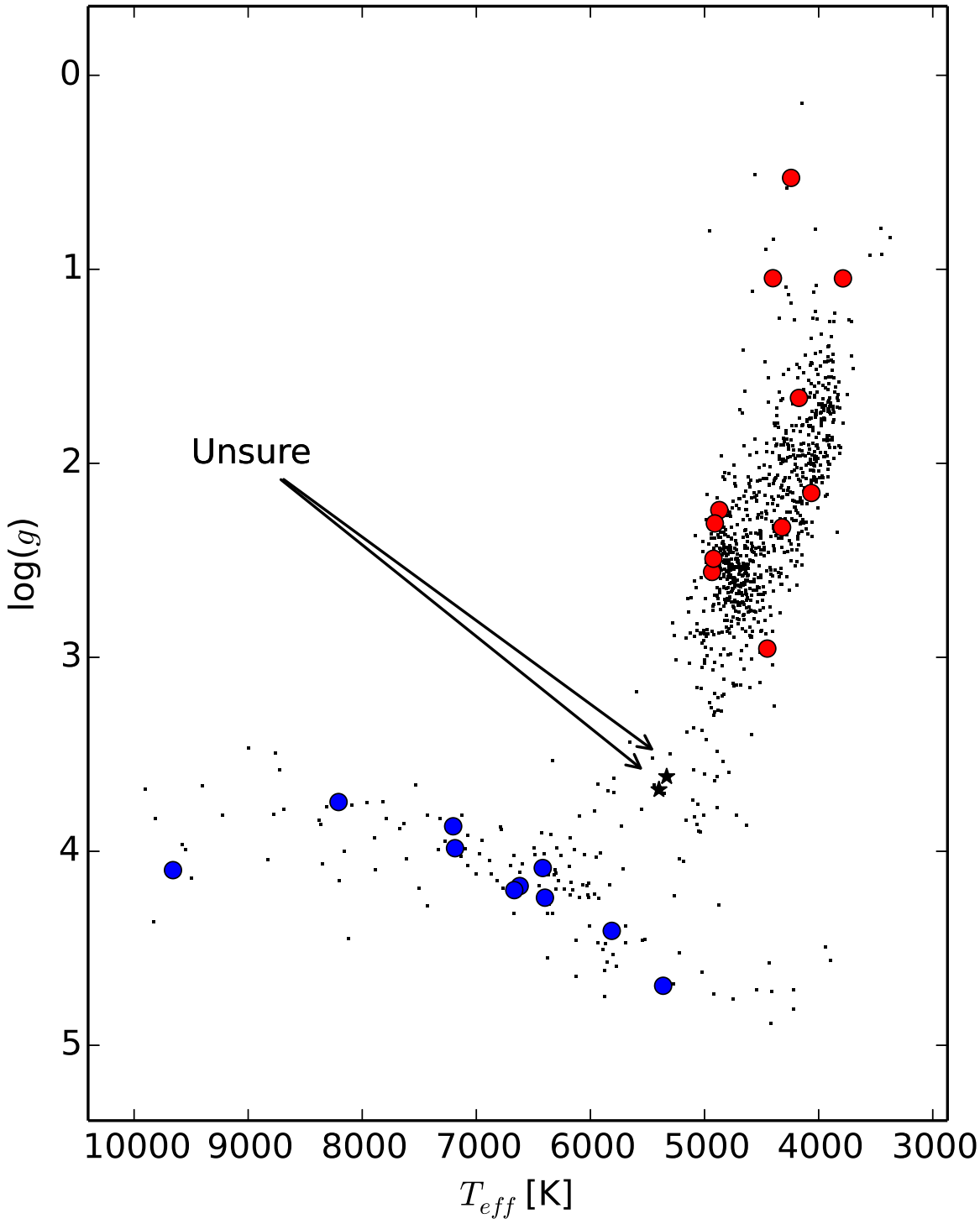

Fig. 3.— H-R Diagram of 22 μm execss stars. Black dots are the more than selected 1000 sources from LAMOST DR1 catalog. Red points are 11 giants, 10 blue points are main sequence stars with mid-infrared excess and 2 black asterisks are unsure.

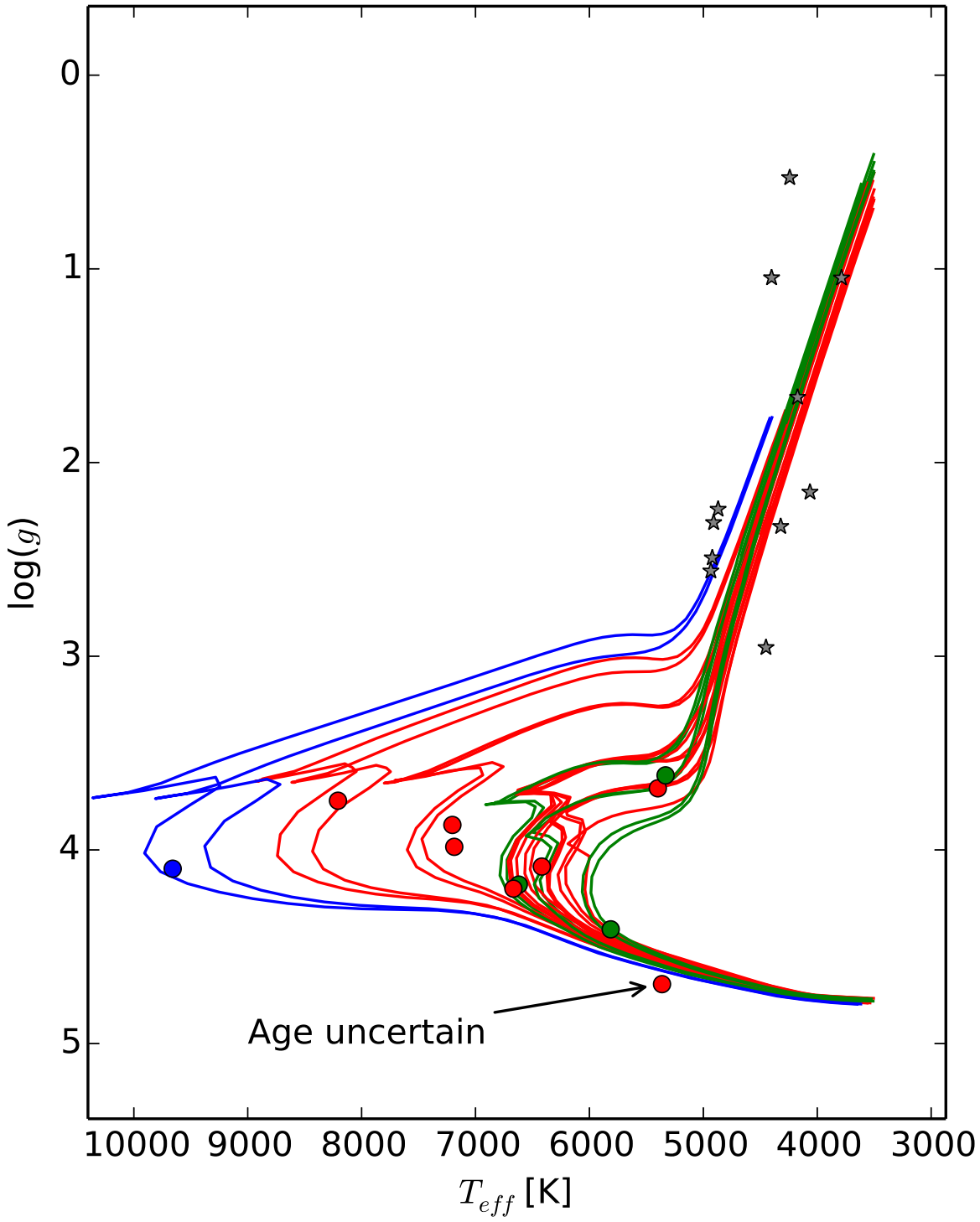

Fig. 4.— Isochrones calculated with [Fe/H]. Symbols with the same color means the same α-enhancement. The corresponding solid lines are plotted for estimating ages.

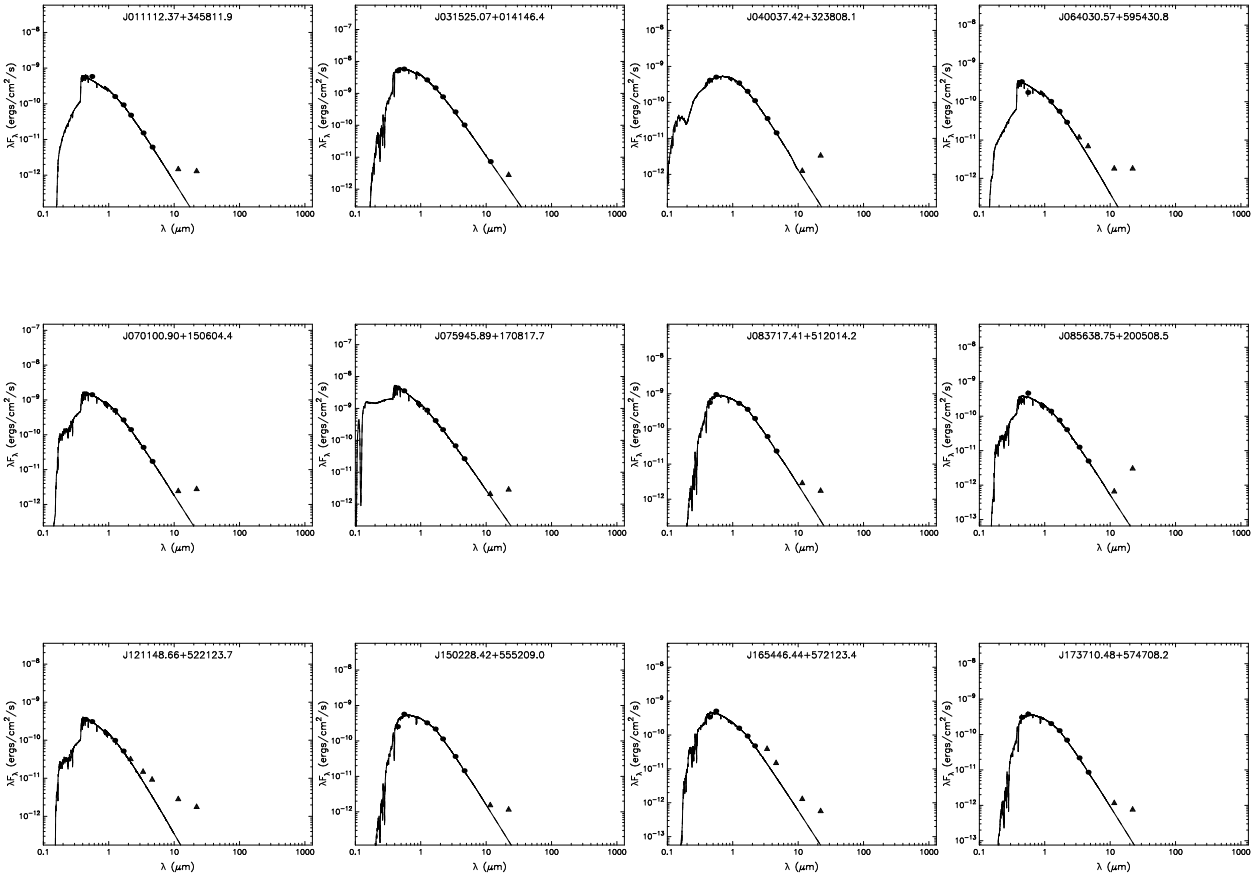

Fig. 5.— The SEDs of 12 candidates. They all almost show excess from 12 μm band. There are 3 show obvious excess from 3.4 μm band and one show slight excess even in the K_s band (J121148.66+522123.7).

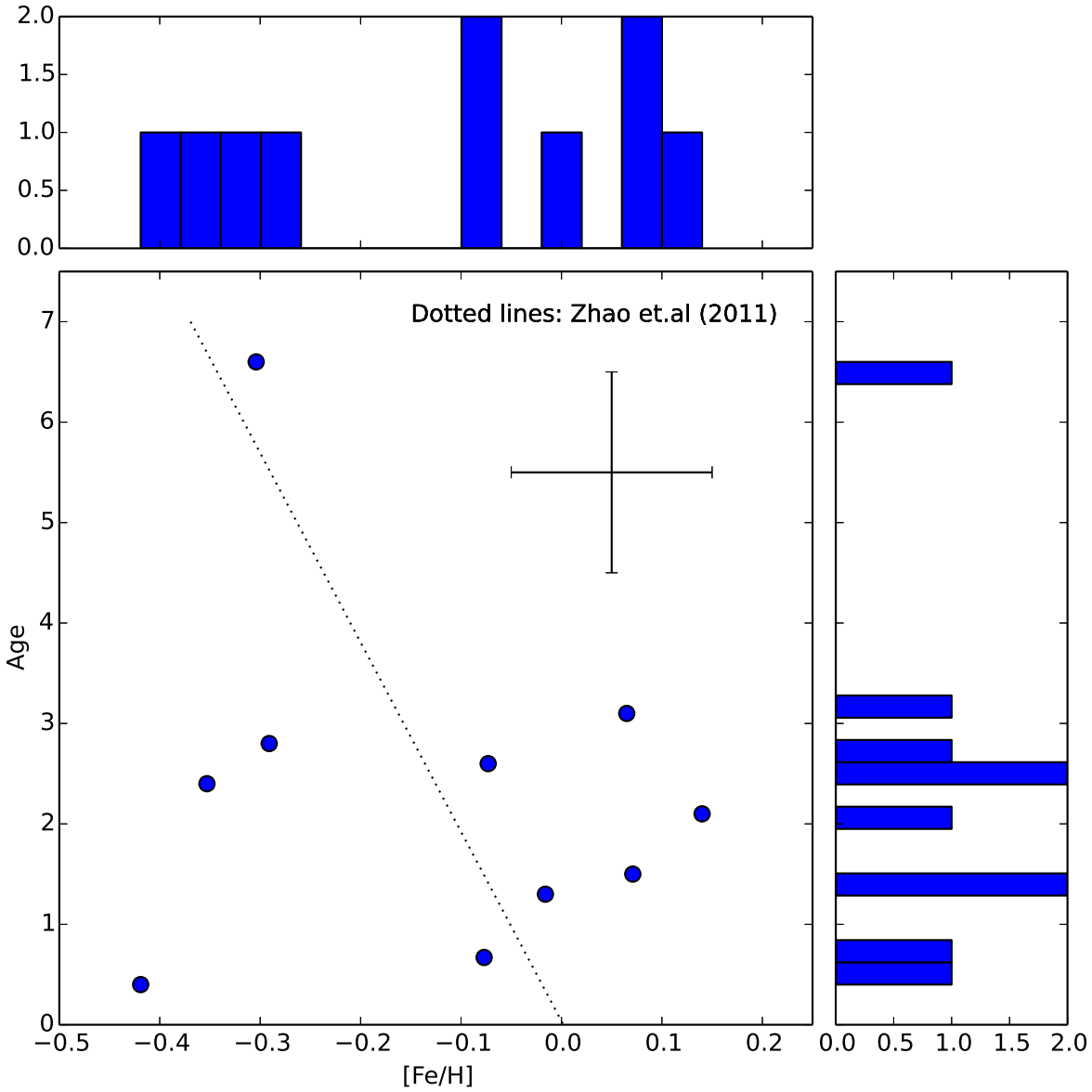

Fig. 6.— Distribution of ages *vs* [Fe/H]. Dotted line shows the relation between age and metallicity for disk stars. The uncertainties are also displayed. There are four stars are metal poor and one (**J173710.48+574708.2**) is metal-poor but with older age.

Table 1. 23 mid-infrared excess stars from LAMOST DR1 Catalog

ID (LAMOST)	RA (J2000)	DEC (J2000)	K-[22]	log g	e_log g	T_{eff} (K)	e_T_{eff}	[Fe/H]	R_v	e_R_v	Age (Gyr)	Note
J010336.21+404117.7	15.90093559	40.68823277	0.443	2.955	0.344	4449.98	40.03	0.232	-37.61	5.16	...	giants
J010354.65+161005.4	15.97773205	16.16819995	0.592	2.153	0.419	4063.76	91.8	-0.083	-4.94	9.04	...	giants
J011112.37+345811.9	17.80160831	34.96996751	3.352	4.179	0.367	6620.3	121.18	-0.353	-42.2	15.05	2.4	F0
J021012.68+122411.7	32.55284506	12.40325597	0.434	2.241	0.795	4870.29	170.29	-0.714	11.84	12.81	...	giants
J031525.07+014146.4	48.85447996	1.69629052	1.159	4.086	0.445	6418.1	135.77	0.14	10.19	10.78	2.1	F5
J040037.42+323808.1	60.1559804	32.63555137	3.459	4.239	0.408	24000.0	109.34	???	11.42	10.99	???	$\sim$ B1
J040851.99-030247.2	62.21664884	-3.04645952	0.52	2.33	0.407	4320.56	64.6	-0.062	30.67	5.9	...	giants
J042431.91-011218.1	66.1329567	-1.20504312	0.45	2.31	0.7	4909.54	89.88	-0.65	43.08	7.72	...	giants
J064030.57+595430.8	100.12746593	59.90860201	4.253	3.871	0.445	7203.22	126.15	-0.016	-11.48	22.76	1.3	F0
J064149.86+553317.1	100.45768452	55.55475347	0.681	1.663	0.43	4172.48	43.5	-0.519	-24.75	6.1	...	giants
J070100.90+150604.4	105.2537717	15.10124246	3.005	3.984	0.375	7186.75	79.56	-0.073	6.91	15.38	2.6	F2
J075945.89+170817.7	119.94119489	17.13827247	2.582	4.097	0.472	9658.87	90.06	-0.419	-9.01	4.81	0.4	A0
J083717.41+512014.2	129.32252087	51.3372757	2.127	4.693	0.406	5362.71	154.25	0.087	2.48	8.29	???	G5
J085638.75+200508.5	134.16135992	20.08574304	4.452	4.2	0.332	6667.45	102.82	0.071	12.96	10.75	1.5	F0
J121148.66+522123.7	182.95277251	52.35662161	4.141	3.746	0.478	8207.83	180.77	-0.077	1.71	21.39	0.67	A3
J150228.42+555209.0	225.61843926	55.86922622	2.294	3.682	0.554	5399.55	90.29	0.065	-41.54	6.69	3.1	F9
J154053.18+500849.1	235.22163025	50.14700443	0.762	2.56	0.926	4933.94	151.35	-1.019	-49.67	15.39	...	giants
J165446.44+572123.4	253.6935751	57.35651971	1.444	3.615	0.643	5331.69	106.01	-0.291	-44.1	9.21	2.8	F9
J165809.02+295451.1	254.53765209	29.91421724	2.386	2.492	0.71	4921.59	106.55	-0.549	-54.03	9.26	...	giants
J171046.48+291418.6	257.69367032	29.23851234	0.476	1.047	0.356	3786.78	24.91	-0.167	2.44	6.18	...	giants
J173710.48+574708.2	264.29373343	57.78558363	2.37	4.41	0.499	5813.22	123.09	-0.304	28.99	9.85	6.6	F9
J191117.64+435907.2	287.8235892	43.98538885	0.483	1.046	0.592	4400.66	54.77	-1.448	-318.42	7.61	...	giants
J194149.90+491728.1	295.45793644	49.29115707	0.483	0.529	0.355	4241.47	40.0	-1.409	-183.96	6.59	...	giants

Table 1—Continued

ID (LAMOST)	RA (J2000)	DEC (J2000)	K-[22]	log g	e_log g	T_{eff} (K)	e_T_{eff}	[Fe/H]	R_v	e_R_v	Age (Gyr)	Note